Nucleic Acids Research, 1997, Vol. 25, No. 18 **3615–3620**

Kinetics of phosphorothioate oligonucleotide metabolism in biological fluids

M. Gilar, A. Belenky, D. L. Smisek, A. Bourque and A. S. Cohen*

Hybridon, Inc., 620 Memorial Drive, Cambridge, MA 02139, USA

Received June 3, 1997; Revised and Accepted August 4, 1997

ABSTRACT

The *in vitro* stability and metabolism of GEM®91, a 25mer phosphorothioate antisense oligonucleotide complementary to the *gag* mRNA region of HIV-1, was investigated using capillary electrophoresis (CE). The *in vitro* degradation of the parent compound at 37°C was followed over the course of 120 h in human plasma. A CE method using laser-induced fluorescence detection was able to detect 5′-end intact metabolites including the parent compound extracted from biological fluids. Because the primary metabolic pathway is believed to be via 3′-exonuclease activity, the results of this study were compared with the stability of the compound in a solution containing 3′-exonuclease. The numerical solution of sequential first-order reactions was used to obtain kinetic parameters. Exonuclease digestion of the parent compound, as measured using an automated CE-UV instrument, yielded striking similarities between the two *in vitro* systems as well as between *in vitro* and *in vivo* systems.

INTRODUCTION

A new era of genetic medicine promises to combat disease at the genetic level. One antiviral approach uses chemically modified oligodeoxyribonucleotides as antisense agents that hybridize specifically to a target mRNA sequence resulting in the suppression of mRNA translation to the corresponding protein and thus virus reproduction (1). The mechanism of antisense action was first described by Zamecnik and Stephenson (2). Zamecnik *et al.* (3) were also first to report an antisense approach to inhibit *de novo* infection by HIV-1 using an unmodified oligodeoxyribonucleotide (ODN). For successful therapeutic use, the *in vivo* stability as well as the bioavailability of antisense compounds is crucial. Sulfurization of ODNs is a frequently used approach to increase *in vivo* stability. The resulting phosphorothioate analogs (SODNs) are more resistant to exonucleases than the unmodified phosphodiester ODNs (4). Even though this modification is one of the most conservative, the chemical properties of a phosphorothioate molecule are different from its phosphodiester counterpart. For example, because of increased charge delocalization, phosphorothioates have a lower pK_a than phosphodiesters (5); phosphorothioates are also more hydrophobic and therefore exhibit more complex secondary structure. Also, the distribution of phosphorothioates in the living organism can be different due to higher binding to proteins and accumulation in organs (6).

As more antisense compounds enter human clinical trials, it becomes increasingly important to obtain a fundamental understanding of the kinetics of degradation and metabolism both *in vitro* and *in vivo*. To establish a baseline for further study, we have investigated the *in vitro* stability and metabolism of GEM®91, a 25mer phosphorothioate antisense oligonucleotide complementary to the *gag* mRNA region of HIV-1, using capillary electrophoresis (CE).

Several papers have been published on *in vivo* and *in vitro* stability and pharmacokinetics of phosphorothioate antisense oligonucleotides. Phosphorothioates were found to be stable with little or no metabolism (7). Most of these studies used radioisotope labeled ^{32}P, ^{35}S or ^{14}C phosphorothioate oligonucleotides. Slab gel electrophoresis on polyacrylamide gels was used for separation of SODN metabolites with radioisotope detection to estimate the metabolites; however, quantification was very poor. Measurements of SODN stability by radioisotope methods sum not only the parent drug radioactivity but also the radioactivity of shorter metabolites and even free isotopes. Precise measurement of parent SODN stability depends on the reliability and sensitivity of the analytical method used for drug level monitoring. To avoid the disadvantages associated with radioisotope methods, we developed a non-radioisotope method for monitoring SODNs in biological fluids using CE with laser-induced fluorescence detection (CE-LIF) with fluorescently-labeled target compounds (8).

Because the primary metabolic pathway in plasma is believed to be by 3′-end exonuclease activity, experiments were conducted both in human plasma and in a solution containing 3′-exonuclease. Our CE-LIF method detects 5′-end intact metabolites including the parent compound from biological fluids. We also developed a CE method with UV detection (CE-UV) that detects both 3′- and 5′-end digested metabolites. For comparison, an unmodified ODN with the same sequence as GEM®91 was run under similar conditions. The kinetics of enzymatic degradation was modeled using a numerical solution of sequential first-order reactions and calculated results compared to measured *in vitro* digestion data.

MATERIALS AND METHODS

Chemical and reagents

Water and methanol were HPLC grade (J. T. Baker, Inc., Phillipsburg, NJ, USA). Human plasma/serum (male) was obtained from Sigma Chemical (St Louis, MO, USA). Uniflo®

*To whom correspondence should be addressed. Tel: +1 617 528 7000; Fax: +1 617 528 7790; Email: acohen@hybridon.com

13 mm diameter 0.2 µm cellulose triacetate disposable syringe filters were obtained from Schleicher and Schuell (Keene, NH, USA). Solid-phase extraction (SPE) was performed on silica based weak anion exchange media in a 2 ml SPE tube (Nucleobond AX-5 cartridges, Macherey Nagel Corp., GmbH & Co., Düren, Germany) and silica based reverse phase C18 media in a 1 ml SPE tube (LC-18, Supelco Corp., Bellefonte, PA, USA). Oligomer HPLC purification was performed on Nucleopak PA-100, 250 × 9 mm column (Dionex, Sunnyvale, CA, USA) and polystyrene–divinylbenzene PRP-3, 150 × 4.1 mm column (Hamilton, Reno, NV, USA). Lithium bromide and other chemicals were obtained from Fluka Chemical Corp. (Ronkonkoma, NY, USA). Deionized formamide was purchased from American Bioanalytical (Natick, MA, USA). Phosphodiesterase I, a 3′ to 5′-exonuclease enzyme isolated from bovine intestinal mucosa, was obtained from Sigma (St Louis, MO, USA).

The 25mer ODN and SODN were synthesized in our lab with an Expedite™ 8909 NASS synthesizer (PerSeptive Biosystems, Framingham, MA, USA), deprotected, purified and reconstituted in deionized water. Fluorescently labeled primer was obtained from Applied Biosystems (Foster City, CA, USA); T4 DNA ligase and ligase buffer (C#202S) and T4 Kinase (C#201S) were obtained from New England Biolabs (Beverly, MA, USA).

Sample preparation and reaction conditions

Human plasma. Plasma samples spiked with ODN were incubated at 37°C. Aliquots were diluted 1:1 with 0.2 M Tris-PO_4, pH 6.3 (EQ), spiked with internal standard, and loaded onto an equilibrated anion exchange (AE) SPE column. The column was washed with 1 × 0.5 ml EQ, 3 × 0.5 ml of 0.2 M NaBr, 0.1 M Tris-PO_4, pH 6.3 in 50% formamide (W1), 1 × 0.5 ml of 0.2 M NaBr, 0.1 M Tris-Cl, pH 7.0 (W2) and 1 × 0.2 ml of 2 M NaBr, 0.1M Tris-Cl (pH 8.5) in 10% isopropanol (E1). A 1.5 ml Eppendorf vial was placed under the SPE tube and 1 × 0.5 m of E1 was added. Because the eluate contained a high ionic strength solution which can suppress electrokinetic CE injection, AE-SPE extracts were desalted using reversed phase SPE as follows. The samples were diluted 1:1 with a 2 M triethylammonium acetate (TEAA) solution (pH 7.0) and loaded onto a conditioned C18 cartridge. The cartridge was washed with 2 × 0.5 ml of 0.1 M TEAA, 1 × 0.5 ml 5% ACN, and the DNA was eluted with 1 × 0.5 ml 40% ACN. The extract was lyophilized, reconstituted in 20 µl of 10 mM NaOH and dialyzed by drop dialysis for 60 min over water using Millipore 0.025 µm membranes. Dialyzed samples were subjected to CE.

Plasma samples containing SODNs were left to react at 37°C. The reaction was stopped by freezing, and samples were stored at –20°C. Samples were diluted 10-fold with water and spiked with 30mer internal standard. Samples were then purified from plasma by SPE. A fluorescently-labeled 17mer primer was ligated to the intact 5′-end of the fragments present in the sample including the parent compound. The labeling has two consecutive steps: phosphorylation of the 5′-end of the oligonucleotide sample followed by ligation of the phosphorylated sample with the fluorescently-labeled primer. A more detailed protocol was presented earlier (8). Ligation occurs only when the bridge DNA hybridizes to a target oligonucleotide whose 5′-end is intact (Fig. 1). Any incompatibility at the 5′-end of the target oligonucleotide with the complementary bridge will prevent ligation to the fluorescent primer. As a result, fluorescently-labeled SODN fragments which differ by one base (due to 3′-end digestion only) can be detected and analyzed at the parts-per-billion level by CE-LIF.

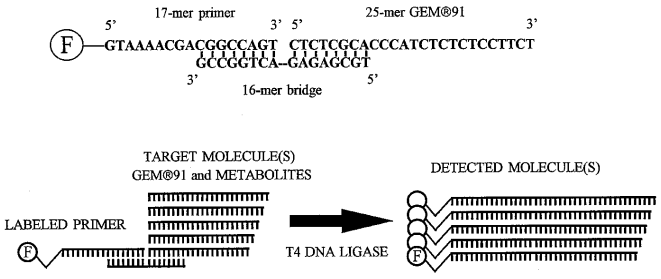

Figure 1. Schematic of ligation procedure. GEM® 91 and its metabolites are ligated with a DNA primer carrying a fluorescent group using a bridge with a complementary sequence. Target molecules are ligated only if they have the 5′-end intact. Detected molecules have identical fluorescence, independent of oligomer chain length.

3′-exonuclease solution. Phosphodiesterase I (from bovine intestinal mucosa) stock solution was prepared in 25 mM Tris–boric acid buffer pH 7.4 to reach the desired concentration of 8.33 nM (0.001 U) of enzyme. This concentration was chosen such that the reaction rate for ODN would be similar to the *in vitro* rate in plasma. Diluting the enzyme in 25 mM Tris–boric acid buffer pH 7.4 kept reaction conditions constant. No dialysis prior to injection was necessary. The same concentration of SODN and ODN (1.3 µM) was used for the reaction in plasma. To determine how the rate of metabolism of the 3′-exonuclease solution depends on ionic strength, the same concentration of enzyme was dissolved in 150 mM NaCl (pH ~7.0). Aliquots of the reaction mixture were immediately heated to 94°C for 5 min to stop the reaction. Samples were dialyzed for 1 h before electrokinetic injection into the CE-UV system. Separation was performed using a replaceable polymer matrix.

Capillary electrophoresis

CE-LIF. Fluorescently-labeled samples were run on a modular CE system with LIF detection (8). An Argon-ion laser (Model 543 100 BS, Omnichrom, Chino, CA, USA) was employed. A 30 kV, 500 µA direct-current high-voltage power supply (Model ER/DM; Glassman, Whitehouse Station, NJ, USA) was used to generate the potential across the capillary. Samples were injected electrokinetically, 10 kV for 2–5 s and then run at 10 kV. Linear polyacrylamide-filled capillaries were prepared in-house by the following manner. Fused-silica capillary tubing (Polymicro Technologies, Phoenix, AZ, USA) with inner diameter of 75 µm, outer diameter of 375 µm, effective length of 10–15 cm, and total length of 27 cm was bifunctionalized with (methylacryloxypropyl) trimethoxysilane (Petrarch Systems, Bristol, PA, USA) and then filled with a degassed solution of 15% polymerizing linear acrylamide in 15% (v/v) formamide media (0.2 M Tris–borate, 2.5 mM EDTA-2Na^+ buffer, pH 8.3, containing 7 M urea). Polymerization was achieved using ammonium persulfate/TEMED chemistry. An electric field of 400–500 V/cm was applied resulting in a current of 10–15 µA.

CE-UV. A BioFocus® 2000 Capillary Electrophoresis System (BioRad, Hercules, CA, USA) with ultra-violet (UV) detection was used. After each run the polymer solution was replaced. The composition of replaceable polymer solution was as follows.

To 2.2 g of BioRad Dynamic Sieving Polymer was added deionized formamide (4.8 ml), 1.2 ml of 10× Tris–boric acid buffer pH 9 (1 M Tris, 0.3 M boric acid), and 1.2 ml of 8.3 M urea solution in 2× Tris-boric acid buffer (0.2 M Tris, 0.06 M boric acid). The Dynamic Sieving Polymer was dissolved, and the solution was degassed under vacuum. The polymer matrix was stable for a week at 4°C. For analysis a 25 cm (20 cm to detection window) coated capillary, 75 µm I.D. × 375 µm O.D. (BioCap oligonucleotide from BioRad) was used. Capillary filling was automated by applying a high pressure N_2 pulse for 220 s. After each run the capillary was washed with HPLC-grade water. Injection of samples was 8 s electrokinetically at 13 kV, and samples were run at 15 kV. Separation was performed at 35°C with a liquid thermostated column.

Numerical solution of sequential first-order reactions

The metabolism of oligomers from exonuclease activity can be modeled as a series of first-order reactions:

$$25\text{mer} \xrightarrow{k_{25},\,-1\text{mer}} 24\text{mer} \xrightarrow{k_{24},\,-1\text{mer}} 23\text{mer} \xrightarrow{k_{23},\,-1\text{mer}} 22\text{mer}... \qquad \mathbf{1}$$

where k_i is the rate constant. If we start with a 25mer and assume first-order kinetics, the rate of parent compound disappearance during the enzymatic reaction is

$$r = -\frac{dc_{25}}{dt} = c_{25}k_{25} \qquad \mathbf{2}$$

where c_{25} is the concentration of 25mer, k_{25} is the rate constant and t is time. The concentration profile of 25mer as a function of time was solved numerically as:

$$c^{i}_{25} = c^{i-1}_{25} + (\mathrm{d}c^{i}_{25}) - \mathrm{d}c^{i}_{25} = k_{25}c^{i}_{25}\mathrm{d}t \qquad \mathbf{3}$$

The actual concentration c^{i}_{25} in the first step is equal to c^{0}_{25}, and due to a gradually decreasing c^{i}_{25} value, the concentration step $\mathrm{d}c_{25}$ decreases exponentially with time. For simplicity the integration step dt was chosen as 1 min and the index number i = 1, 2, 3.... Similar calculations were performed to compute the concentration of shorter products noting that the rate of 25mer disappearance $\mathrm{d}c_{25}$ is equal to the rate of 24mer appearance $\mathrm{d}c_{24}$ etc. The calculations were performed using a Microsoft Excel spreadsheet assuming that the kinetic constant k_{25} is equal to the kinetic constants of subsequent reactions of shorter metabolites ($k_{25} = k_{24} = k_{23}$...).

Data quantitation

Quantitation was performed using an internal standard and using a method of internal normalization. Internal normalization was based on the assumption that the sum of all SODN fragments peak height is proportional to the spiked molar concentration:

$$c_{sp} = \sum c_i \approx H_{sp} = \sum H_i \qquad \mathbf{4}$$

where H_i is the peak height of SODN fragments and c_{sp} is the spiked concentration of SODN 25mer. Summation of peak heights was possible using LIF detection because of a homoextinction response of SODN fragments from the detector where each fragment at the same molar concentration gives the same signal. The concentrations of the SODN parent compound and metabolism products were calculated as:

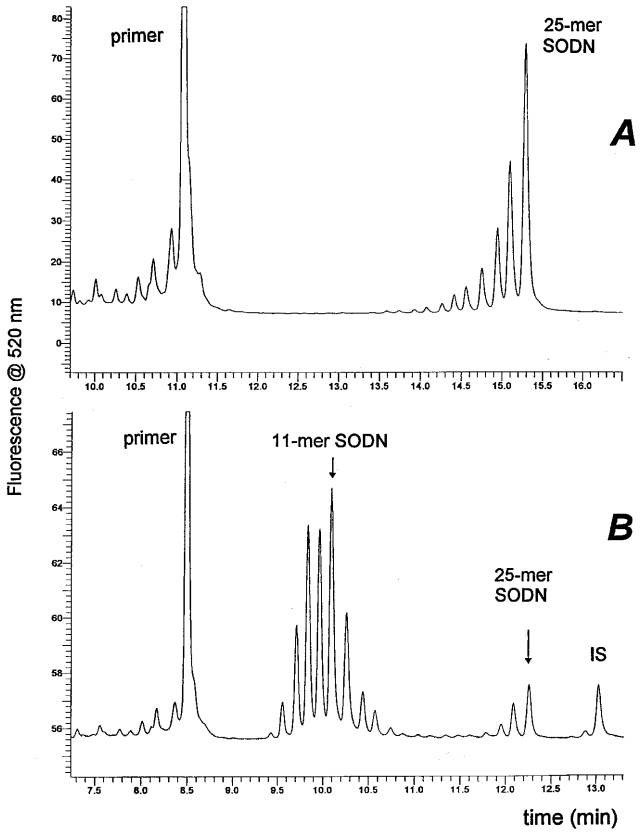

Figure 2. *In vivo* metabolism of GEM® 91 after single dose (primate). (**A**) Plasma metabolite profile 6 h after single intravenous dose. (**B**) Urine metabolite profile, urine collected from 0 to 6 h.

$$c_i = \frac{H_i}{\sum H_i} \times c_{sp} \qquad \mathbf{5}$$

We assume that the efficiency of fluorescent labeling (ligation with fluorescent primer) is equal for each SODN fragment and the digestion of SODN from the 5′-end can be neglected. In our experience the shape and efficiency of closely migrating peaks do not significantly differ, and the internal normalization method gave better results than the results obtained by internal standard only.

RESULTS AND DISCUSSION

Enzymatic degradation from the 3′-end is a main metabolic pathway of SODNs both *in vivo* and *in vitro*. In our experience characteristic 3′-end metabolite profiles from *in vivo* experiments can be found in plasma and in urine following a single dose (Fig. 2). While ODNs are quickly metabolized and present in plasma mainly as short oligonucleotides or nucleotides, SODNs are mainly non-metabolized in plasma, and the parent compound is present all the time *in vivo* forming a characteristic ‘right triangle’ shaped metabolic profile (Fig. 2A). This behavior can be related to greater SODN stability and to accumulation in tissue (9). Slow release of parent SODN (and its first metabolites) accumulated in tissue was observed by several authors who fitted the pharmacokinetcs of body drug clearance with a two-compartmental model (10,11). *In vitro* metabolism of SODNs in human plasma gave a very similar metabolite profile of 3′-exonuclease cleavage products (Fig. 3B) to what was found *in vivo*.

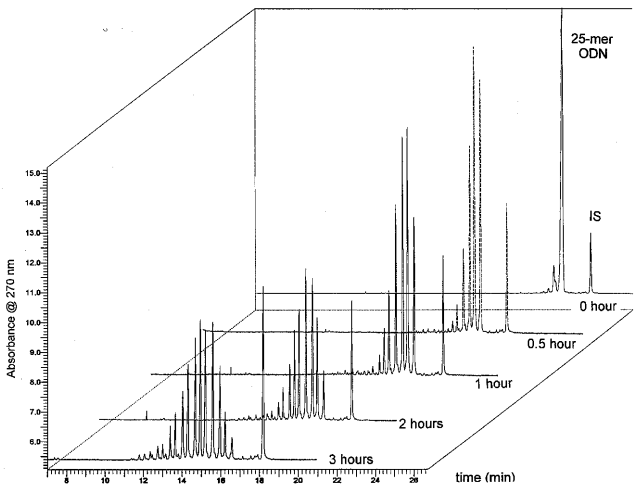

Figure 3. *In vitro* plasma metabolism of (**A**) 25mer ODN and (**B**) 25mer SODN (GEM®91). The parent SODN oligonucleotide and corresponding metabolites were analyzed using CE-LIF with a linear polyacrylamide matrix. IS denotes internal standard.

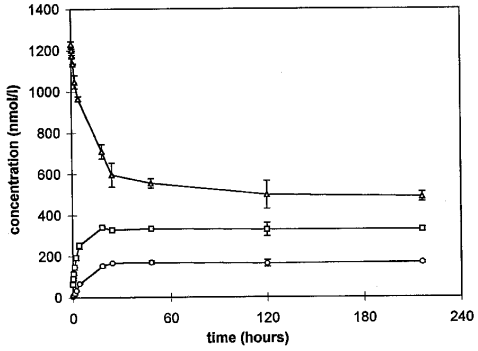

Figure 4. Concentrations of 25mer (triangles), 24mer (squares) and 23mer (circles) SODNs in plasma during *in vitro* metabolism. Fresh human plasma was spiked with 1.3 μM 25mer SODN and incubated at 37°C. Aliquots were taken at 0, 0.25, 0.5, 1, 2, 4, 18, 24, 48, 120 and 216 h.

Comparison of the *in vitro* metabolism of SODNs and ODNs of the same sequence emphasizes the greater phosphorothioate stability (Fig. 3). The ODN concentration in plasma and other reaction conditions were kept identical to that of the SODN digestion. Quantification was performed according to the internal normalization method (equation **5**). Because UV detection depends on the extinction coefficient of ODN fragments, $Hred_i$ ($\Sigma Hred_i$) was used in equation **5** instead of H_i (ΣH_i) where $Hred_i = H_i/\varepsilon_i$. The theoretical molar extinction coefficient of i-mer, ε_i, was calculated according to

$$\varepsilon_I = aA + bG + cC + dT$$

where *A* (adenosine), *G* (guanine), *C* (cytosine) and *T* (thymine) are base molar absorptivity values (11170, 11875, 9161 and 7872, respectively) and *a*, *b*, *c* and *d* are the number of each respective base in the DNA molecule. The calculated kinetic constant for ODN 25mer disappearance was $k = 1.8\ h^{-1}$ ($t_{1/2} = 0.39$ h). When this kinetic constant was used for first-order kinetic numerical modeling of the metabolic profile, agreement was obtained between the measured and modeled data for the first three metabolites (data not shown). ODN enzymatic hydrolysis generates a characteristic 'Gaussian' profile of metabolites as illustrated on the electropherograms of Figure 3A.

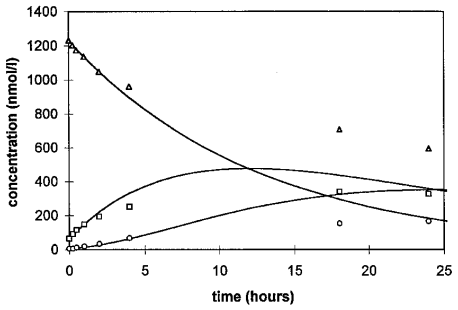

Figure 5. Comparison of calculated concentrations (smooth lines) of parent SODN and the first two metabolites (24- and 23mers) with measured plasma concentrations of 25mer (triangles), 24mer (squares) and 23mer (circles).

Figure 4 shows the concentration profile of parent compound (25mer) and the first two metabolites (24- and 23mer) using CE-LIF. As can be seen from the figure, the reaction runs faster in the beginning, later slows down, and then nearly stops after ~24 h. This decreased reaction rate is apparent from the leveling of concentration of the 25mer parent compound and first two metabolites.

To assess if the reaction follows first-order kinetics and to obtain the kinetic rate constant, we calculated the change in 25mer concentration with time. On a logarithm scale we observe that the reaction rate is not constant over the course of the experiment; however, a good linear fit is found in the range of 0–2 h (correlation coefficient, $r_{x,y} = 0.9989$). The kinetic constant calculated from this interval, $k = 0.0792\ h^{-1}$, yields a half-life value of $t_{1/2} = 8.75$ h. As a check of this constant, we compared the measured data of the 25-, 24- and 23mer with the calculated results. Figure 5 shows an overlay of the measured and calculated data. Perfect agreement is expected for the 25mer in the range of 0–2 h because those data were used to calculate the kinetic constant. Excellent agreement between the measured and calculated data for the 24- and 23mer supports first-order kinetics during this time period.

Figure 6 shows a plot of the concentration of SODN 25mer and its 24- and 23mer metabolites versus time. These concentration profiles are similar to those obtained in plasma (Fig. 4). As in plasma, a gradually decreasing reaction rate was found for SODNs in the 3′-exonuclease solution. This *in vitro* plasma digestion data of SODNs leads us to speculate why the reaction rate decreased during SODN metabolism and why the reaction deviated from first-order kinetics after only 2 h. This finding can be explained by several hypotheses.

I. The 3′-exonucleases are not stable in plasma; their activity during the reaction gradually decreases. This process significantly influences long-term SODN metabolism while having a negligible effect on the ODN reaction. To test the stability of the enzyme in plasma, fresh plasma was left at 37°C for 18 h. The plasma was then spiked with the same amount (1.3 μM) of SODN as in the experiment using fresh plasma with no prior incubation time. The reaction rate after 1 h was compared to the rate in fresh plasma with no prior incubation time. As a criterion the ratio H_{25mer}/H_{24mer} was used. For fresh plasma H_{25mer}/H_{24mer} was assumed to equal 100% of the reaction rate. A value of 71% of the rate reaction in plasma was found after 18 h at 37°C. A much lower value (~25%)

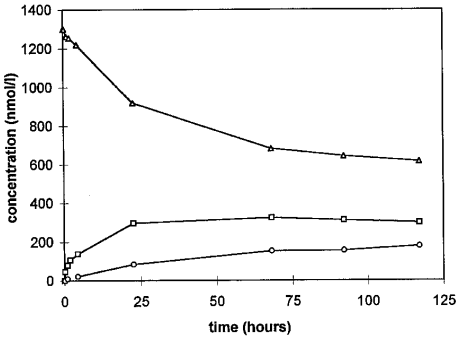

Figure 6. Concentrations of 25mer (triangles), 24mer (squares) and 23mer (circles) during *in vitro* metabolism in the 3′-exonuclease solution (8.33 nM 3′-exonuclease in 25 mM Tris–boric acid buffer, pH 7.4). Concentrations of SODNs were measured by CE-UV with a replaceable polymer matrix.

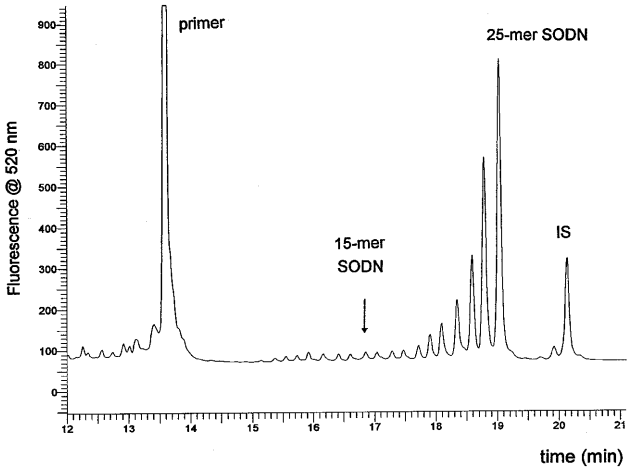

Figure 7. *In vitro* plasma metabolism of GEM®91 after 216 h. IS denotes internal standard.

should be found if enzyme decomposition is responsible for the decreased reaction rate.

To exclude the possibility that the decomposition of the enzyme is responsible for the decreasing SODN reaction rate, enzyme stability was also tested in the 3′-exonuclease solution. The prepared enzyme solution (8.33 nM) was divided into three vials and stored at 20°C before the addition of ODN. Enzyme stability was determined from the reaction rate of the 25mer ODN (Table 1).

Only a slight decrease in enzyme activity was found after 90 h. This finding does not correlate with the decreasing SODN reaction rate. Even if we assume partial enzyme decomposition, this effect could not explain the formation of the ‘right triangle’ shaped profile. From Figures 4 and 6 it follows that after 60 h a very slow reaction can be observed for the 25mer, and the concentration of the first two metabolites is virtually constant. Despite this fact, new shorter metabolites gradually appear on the electropherogram out to 216 h in plasma. The subsequent production of shorter fragments is slow, but significant (Fig. 7). Similar behavior can also be seen during metabolism in the 3′-exonuclease solution (Fig. 8). Our experiments do not give us a clear explanation of this finding.

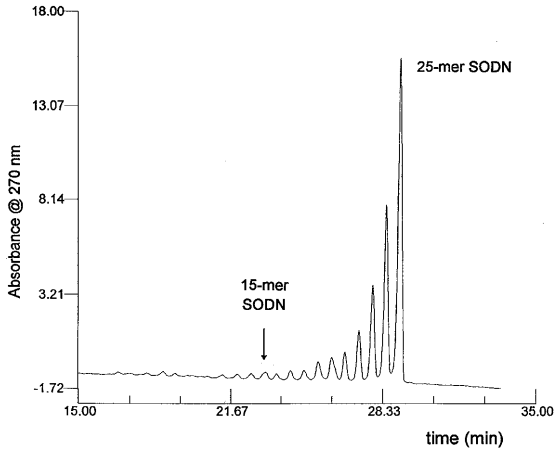

Figure 8. *In vitro* metabolism of GEM®91 in 83.3 nM 3′-exonuclease solution after 48 h. For other conditions see Materials and Methods.

Table 1. Enzyme stability at 20°C measured as half-lives of 25mer ODN metabolism

Time of enzyme at 20°C before ODN addition (h)	Half-life of 25mer ODN metabolism (h)
0	0.27
6	0.28
90	0.32

II. The assumption of first-order reaction rate is incorrect for SODNs. Because of a relatively high excess of SODN substrate versus enzyme molar concentration (154:1), the enzyme could be saturated. This behavior is significant for SODNs if we suppose that they are more strongly bound to the enzyme than ODNs. The SODN reaction kinetics could have an order between 0 and 1st. This assumption, however, does not explain the decrease in reaction rate, and in the case when the reaction order is <1, the dependence of ln concentration versus time will be concave instead convex. The measured data are not fit well by second-order kinetics.

One explanation for the observed kinetics is an inhibition of enzyme by phosphorothioate mononucleotides released from the 3′-end. This possibility was tested experimentally. No significant difference in enzyme activity was found digesting the 25mer ODN in buffer containing mononucleotides generated by previous total hydrolysis of ODN or ODN/SODN oligomers.

III. SODNs are more strongly adsorbed to plasma proteins than ODNs, and therefore the free plasma concentration is limiting the reaction rate. To explain the gradual decrease in reaction rate, the kinetics of plasma protein–SODN binding are assumed to be relatively slow ($t_{1/2}$ of SODN–protein interaction ~ $t_{1/2}$ of metabolism). To compare the *in vitro* plasma metabolism with the metabolism in media not containing a high concentration of proteins, a solution of 3′-exonuclease was prepared in 25 mM Tris–boric acid buffer (pH 7.4). The half-life of the parent ODN in 3′-exonuclease solution was $t_{1/2}$ = 0.27 h. The reaction followed first-order kinetics, and a characteristic ‘Gaussian’ metabolite profile was observed. Despite different reaction temperatures (37°C in plasma and 20°C in the 3′-exonuclease solution), ODN

stability in the 3′-exonuclease solution correlates with plasma stability very well (Table 2). Both the 25 mM Tris–boric acid buffer and the 150 mM NaCl solution show similar ODN stability.

Table 2. Stability of phosphodiester (ODN) and phosphorothioate (SODN) 25mers of identical sequence in plasma and in 3′-exonuclease solution

Reaction medium	Substrate (1.3 nM)	$t_{1/2}$ (h)[a]	SODN $t_{1/2}$/ ODN $t_{1/2}$
Plasma, 37°C	ODN	0.39	
	SODN	8.75	22.44
3′-exonuclease solution	ODN	0.27	
20°C, 25 mM buffer, pH 7.4	SODN	30.50	112.96
3′-exonuclease solution	ODN	0.21	
20°C, 150 mM NaCl, pH 7.0	SODN	5.15	24.52
In vivo plasma, single dose	ODN	0.04[b]	
	SODN	0.2–1.5[c]	

[a]Calculated from first 2 h of reaction (*in vitro*).
[b]Estimated for rabbit, 20mer ODN.
[c]Human, half-life depends on dose.

The half-life for the SODN reaction in 25 mM Tris–boric acid buffer is longer than expected according to plasma metabolism. The SODN reaction in the 3′-exonuclease solution at physiological ionic strength (150 mM NaCl) correlates very well with the plasma results. From this experiment we can conclude that the adsorption of SODNs to the enzyme is stronger than for ODNs, and higher ionic strength can speed up the desorption process more significantly for SODNs. Another explanation is that phosphorothioate oligomers could be adsorbed at low ionic strength to the enzyme surface so strongly as to be able to partially deactivate the enzyme.

A similar right triangle shaped pattern of *in vitro* SODN digestion in plasma was found in the low protein media, which shows that the decreasing reaction rate of SODNs is not a result of interaction with plasma proteins. The ratios between SODN $t_{1/2}$ and ODN $t_{1/2}$ in Table 2 confirms that the 3′-exonuclease solution can successfully model the activity of plasma enzymes in the study of 3′-end metabolism of oligonucleotides.

CONCLUSIONS

The half-lives of SODN and ODN 25mer oligonucleotides (GEM® 91 sequence) were measured both in plasma and in a 3′-exonuclease solution. The *in vitro* enzymatic degradation in plasma and in a 3′-exonuclease solution are similar indicating that the 3′-exonuclease solution can model the plasma medium.

Phosphodiester metabolism in plasma can be described by first-order kinetics while the phosphorothioate followed first-order kinetics in plasma for only 2 h. During the latter reaction, the reaction rate gradually decreased with time and virtually stopped after the formation of a characteristic right triangle shaped metabolite profile. The same pattern of SODN metabolism was found in plasma and in the 3′-exonuclease solution. Enzyme activity was investigated in both media, and good activity was found for >90 h. Enzyme decomposition during the reaction did not explain the observed decreasing reaction rate. The possibility of SODN–plasma protein interaction was also ruled out as a reason for the decreasing reaction rate. The right triangle shaped metabolite profile is very similar to those typically observed *in vivo* in plasma. This fact leads us to speculate that this profile is generated by the nature of the metabolic process and does not necessarily depend on the slow efflux of parent drug and metabolites from tissues.

Using the first 2 h to calculate the first-order kinetic constant shows that the 25mer SODN has more than 20 times greater stability than the corresponding 25mer ODN of the same sequence both in plasma and in the 3′-exonuclease solution. Further study of the mechanism of phosphorothioate resistance to enzymatic hydrolysis is ongoing.

REFERENCES

1 Crooke, S.T. and Lebleu, B. (eds) (1993) *Antisense Research and Applications*. CRC Press, Boca Raton, FL.
2 Zamecnik, P.C. and Stephenson, M.L. (1978) *Proc. Natl. Acad. Sci. USA*, **75**, 280–284.
3 Zamecnik, P.C., Goodchild, J., Taguchi, Y. and Sarin, P.S. (1986) *Proc. Natl. Acad. Sci. USA*, **83**, 4143–4146.
4 Srinivasan, S.K. and Iversen, P. (1995) *J. Clin. Lab. Anal.*, **9**, 129–137.
5 Frey, P.A. and Sammons, R.D. (1985) *Science*, **228**, 541–545.
6 Agrawal, S. (1996) *Trends Biotech.*, **14**, 376–387.
7 Iversen P. (1993) In Crooke, S.T. and Lebleu, B. (eds), *Antisense Research and Applications*. CRC Press, Boca Raton, FL. pp. 461–469.
8 Cohen, A.S., Bourque, A.J., Wang, B.H., Smisek, D.L. and Belenky, A. (1997) *Antisense Nucleic Acid Drug Dev.*, **7**, 13–22.
9 Crooke, S.T., Graham, M.J., Zuckerman, J.E., Brooks, D., Conklin, B.S., Cummins, L.L., Greig, M.J., Guinosso, C.J., Kornbrust, D., Manoharan, M., *et al*. (1996) *J. Pharmacol. Exp. Ther.*, **277**, 923–937.
10 Zhang, R., Diasio, R.B., Lu, Z., Liu, T., Jiang, Z., Galbraith, W. and Agrawal, S. (1995) *Biochem. Pharm.*, **49**, 929–939.
11 Zhang, R., Yan, J., Shahinian, H., Amin, G., Lu, Z., Liu, T., Saag, M.S., Jiang, Z., Temsamani, J., Martin, R.R., *et al*. (1995) *Clin. Pharm. Ther.*, **58**, 44–53.